Characterization of Maya Asphaltene and Maltene by Means of Pyrolysis Application

ARTICLE *in* ENERGY & FUELS · MAY 2008

Impact Factor: 2.79 · DOI: 10.1021/ef800024p

3 AUTHORS, INCLUDING:

J. Douda
Instituto Politécnico Nacional
27 PUBLICATIONS **287** CITATIONS

Characterization of Maya Asphaltene and Maltene by Means of Pyrolysis Application

J. Douda,*,† R. Alvarez,‡ and J. Navarrete Bolaños‡

La Unidad Profesional Interdisciplinaria en Ingeniería y Tecnologías Avanzadas (UPIITA), Instituto Politecnico Nacional, D.F., 07340, Mexico, and Instituto Mexicano del Petróleo (IMP), Eje Central Lázaro Cárdenas 152, D.F., 07730, Mexico

Received January 10, 2008. Revised Manuscript Received March 30, 2008

The comparison of the original Maya asphaltene and asphaltene samples obtained after pyrolysis has been performed by different analytical methods: mass spectrometry, infrared spectroscopy, and ^{13}C solid-state magic-angle spinning−nuclear magnetic resonance (MAS−NMR) spectroscopy. The original asphaltene sample has been studied by solution-state ^{13}C and ^{1}H NMR spectroscopy. Besides, outline pyrolysis of the isolated Maya maltene at $T > 350$ °C was performed. As a result, coke, asphaltene, maltene, and gas products have been obtained. The initial Maya maltene has been studied by thermogravimetric and differential thermal analyses. The results of Maya asphaltene and maltene pyrolysis have been compared and discussed.

Introduction

The study of asphaltene structure and chemical composition and its interaction with the maltene fraction in the oil solution provides important information to prevent the asphaltene flocculation and deposition. One of the ways to avoid asphaltene precipitation is the application of flocculation inhibitors: the compounds with the properties similar to resin molecules, which form a steric repulsive layer around an asphaltene core.[1] That is why knowledge of the structure of asphaltenes and resins plays a crucial role in the design of efficient flocculation inhibitor molecules, which is mainly based on the specific interaction between the inhibitor polar part and asphaltene aromatic core.[2–6]

The pyrolysis application for isolated asphaltene and maltene samples helps to observe the temperature modifications, from which some ideas about the structure of these molecules may be obtained. The method of pyrolysis has been recently applied to study thermal degradation of asphaltene.[3] Pyrolysis reduces the molecular weight of the full-size initial molecules, making possible the analysis of the products.[3,7,8] On the other hand, condensation reactions may occur during pyrolysis.[9,10]

Recently, we have studied the Maya asphaltene pyrolysis at different temperatures by application of thermal gravimetric (TGA) and differential thermal analyses (DTA) and outline pyrolysis methods.[3] The outline technique of pyrolysis (no connected with other analytical equipments) solves the problem of the analysis of heavy compounds, recovery of all pyrolysis products, and storage of samples for subsequent analyses.[11] We reported the percent production of coke, gas, asphaltene, and maltene fractions at pyrolysis temperatures of 350−450 °C.[3] The content and composition of the saturated, aromatic, and polar compounds of the Maya asphaltene pyrolysis were also studied.

Strausz et al.[12] applied the outline pyrolysis method to study structural features of Boscan and Duri asphaltenes. The results of thermal analyses (TGA/DTA) of Garzan and Raman crude oils and their fractions were reported in ref 13. Friesen et al. studied the thermal properties of Athabasca maltene and asphaltene.[14] Very recently, Huang[15] has reported the TGA of Florida asphaltene and concluded that the thermal decomposition and abundant coke production occur primarily between 350 and 450 °C, the temperature range, which is applied in the present study. Also, the asphaltene and its thermally degraded fractions have been characterized by TGA and infrared spectrometry in another work of his.[16] However, analyzed products were not separated by solvent sequence to individual fractions of coke, asphaltene, gas, and maltene, as was performed, for example, in ref 3.

The online technique of pyrolysis−gas chromatography−mass spectrometry (Py−GC−MS) has been applied to the analysis of petroleum vacuum residues[17] and asphaltenes.[18] However, the applied technique did not elute any aromatics in the samples known to be present from size-exclusion chromatograpy (SEC).

* To whom correspondence should be addressed. E-mail: jannaduda@hotmail.com.

† La Unidad Profesional Interdisciplinaria en Ingeniería y Tecnologías Avanzadas (UPIITA).

‡ Instituto Mexicano del Petróleo (IMP).

(1) Kaminski, T. J.; Fogler, H. S.; Wolf, N.; Wattana, P.; Mairal, A. *Energy Fuels* **2000**, *14*, 25.

(2) Murgich, J. *Energy Fuels* **1996**, *10*, 68.

(3) Douda, J.; Llanos, M. E.; Alvarez, R.; López Franco, C.; Montoya de la Fuente, J. A. *J. Anal. Appl. Pyrolysis* **2004**, *71*, 601.

(4) Ortega-Rodriguez, A.; Duda, Y.; Guevara-Rodriguez, F.; Lira-Galeana, C. *Energy Fuels* **2004**, *18*, 674.

(5) (a) Barcenas, M.; Duda, Y. *Phys. Lett. A*, **2007**, *365*, 454. (b) Barcenas, M.; Douda, J.; Duda, Y. *J. Chem. Phys*, 2007, *127*, 114706.

(6) León, O.; Contreras, E.; Rogel, E.; Dambakli, G.; Espidel, J.; Acevedo, S. *Energy Fuels* **2001**, *15*, 1028.

(7) Savage, P. E.; Klein, M. T. *Energy Fuels* **1988**, *2*, 619.

(8) Ancheyta, J.; Centeno, G.; Trejo, F.; Marroguin, G. *Energy Fuels* **2003**, *17*, 1233.

(9) Artok, L.; Su, Y.; Hirose, Y.; Hosokawa, M.; Murata, S.; Nomura, M. *Energy Fuels* **1999**, *13*, 287.

(10) Saydut, A.; Duz, M. Z.; Tonbul, Y.; Baysal, A.; Hamamci, C. *J. Anal. Appl. Pyrolysis* **2008**, *81*, 95.

(11) Douda, J.; Llanos, M. E.; Alvarez, R.; Navarrete Bolaños, J. *Energy Fuels* **2004**, *18*, 736–742.

(12) Strausz, O. P.; Mojelsky, T. W.; Lown, E. M. *Energy Fuels* **1999**, *13*, 228–247.

(13) Karacan, O.; Kok, M. V. *Energy Fuels* **1997**, *11*, 385.

(14) Friesen, W. I.; Michaelian, K. H.; Long, Y.; Dabros, T. *Energy Fuels* **2005**, *19*, 1109.

(15) Huang, J. *Pet. Sci. Technol.* **2007**, *25*, 1313.

(16) Huang, J. *Pet. Sci. Technol.* **2006**, *24*, 1089.

10.1021/ef800024p CCC: $40.75
Published on Web 05/17/2008

Table 1. Product Yields of Maya Asphaltene[3] and Maltene Pyrolysis at Different Temperatures

products (%)	B 350 °C	C 350 °C	Cm 350 °C	D 400 °C	Dm 400 °C	E 450 °C	Em 450 °C
coke	24.8	35.5	0.4	57.7	0.5	72.5	5.2
gas	0.5	0.6	13.4	19.0	10.7	7.9	17.5
asphaltene	68.2	52.5	0.9	11.4	4.4	0.6	3.5
maltene	6.5	11.4	85.3	11.9	84.3	19.0	73.7
total solids	99.5	99.4	86.6	81.0	89.3	92.1	82.5

Trejo and Ancheyta[19] have reported the results of SEC fractionation of asphaltenes from the hydrotreated Maya crude oil by elemental analysis, metal content, and matrix-assisted laser desorption ionization mass spectrometry (MALDI−MS). They have found that the molecular-weight distribution of asphaltenes from hydrotreated Maya crude oil was decreased as a consequence of the high severity of reaction conditions (namely, 380−420 °C and pressures of 70−100 kg/cm^2).

The pyrolysis of Arabian Light maltene at 425 °C was reported by Yasar et al.;[20] they indicated that the asphaltene and coke were formed in series: maltene → asphaltene → coke. The reason for coke formation in fuels has been associated with the poor thermal stability of long-chain alkanes,[21] and some pathways of solid formation have been discussed.[22]

The thermal decomposition of petroleum asphaltenes has received some attention, but special interest has been devoted to the nature of the volatile products of asphaltene decomposition mainly because of the difficulty of characterizing the nonvolatile coke.[23] The outline kind of pyrolysis of asphaltene and maltene applied in the present study amplified the possibilities to recovery, storage, fractionation, and analysis of nonvolatile products. With few exceptions mentioned above, the outline pyrolysis of asphaltene and maltene has not been reported in the literature to the best of our knowledge.

It is obvious that, to have a complete idea about the asphaltene structure, the study of the initial sample alone is not enough. Thus, in this work, our aim is to compare the original asphaltene sample with the asphaltene fractions obtained after pyrolysis at 350, 400, and 450 °C. The unreacted asphaltene products of the Maya asphaltene pyrolysis collected at 350−450 °C are evaluated. The samples of initial Maya asphaltene and unreacted asphaltene products are analyzed by means of electron ionization mass spectrometry (EIMS), Fourier transform infrared spectroscopy (FTIR), ^{13}C magic-angle spinning−nuclear magnetic resonance (MAS−NMR), and solution-state ^{1}H and ^{13}C NMR spectroscopy. All of these analytical techniques have been recently shown to be useful for the characterization of asphaltenes and pyrolized asphaltenes.[24–27]

On another hand, we study the Maya maltene thermal degradation to determine the yields of maltene pyrolysis products (coke, asphaltene, gas, and unreacted maltene) at mild temperatures, T = 350, 400, and 450 °C. Thermogravimetric and differential thermal analyses of the original maltene sample are applied to study the changes that occur in this sample at temperatures up to 996 °C.

Experimental Procedure

A Maya crude oil has been obtained from the Mexican Petroleum Company (PEMEX). The experimental procedure of precipitation of asphaltene is described in our previous works.[3,11] Briefly, it was added 40:1 (v/v) excess of *n*-heptane to crude oil, and the suspension was stirred for 1 h, settled overnight, and filtered. The *n*-heptane-soluble fraction yields an initial maltene sample. The precipitate was dissolved in toluene at a ratio of 20:1, filtered, concentrated, and reprecipitated (40:1 excess of *n*-heptane). The reprecipitated asphaltene was subjected to Soxhlet extraction with *n*-heptane for 40 h.

The experiments of outline pyrolysis were performed using a specially constructed device described in ref 3. Briefly, the quartz tube reactor (30 mm in outer diameter and 0.65 m in length) was installed into an electric Thermolyne 79300 tube furnace with the temperature and pressure controlled and flushed with a constant flow of nitrogen at normal pressure. The pyrolysis products were transported to ice-cooled and water traps. When the reactor temperature was equilibrated at 350, 400, and 450 °C, the reactor was disconnected; the asphaltene (or maltene) sample was removed inside the hot zone of the reactor in a special container. Immediately, the reactor was connected again, kept at the given reaction temperatures during 30 (or 20 min), and then gradually cooled to room temperature. The sublimated fraction was extracted with dichloromethane to yield a coke (dichloromethane-insoluble solid) and asphaltene (dichloromethane-soluble solid).

The porphyrin sample was obtained from original Maya asphaltene:[28] a sample was dissolved in methylene chloride and transferred to a silica-gel-packed column. Porphyrins were eluted using a gradient of solvents: starting with acetone (100%) and followed by a mixture of acetone/methylene chloride, until a final concentration of 50:50 (v/v) was reached. The solids obtained after solvent evaporation were transferred to a sealed vial and stored in the dark at 4 °C.

For EIMS analysis, the pyrolyzed asphaltene and porphyrin samples were dissolved in dichloromethane and then analyzed with a Jeol mass spectrometer (JMS-AX 505 WA). The direct introduction of the samples and electron ionization energy of 70 eV were used. The temperature of EIMS analysis was 350 °C.

The FTIR analysis of asphaltene samples was carried out using KBr wafers, where asphaltene was diluted at 2 wt % with spectrophotometric-grade potassium bromide salt. The obtained 13 mm pellet was mounted on a sample holder and then analyzed in a Nicolet model 710 spectrophotometer in the absorbance mode with a resolution of 4 cm^{-1} and 100 scans in the medium IR range (4000−400 cm^{-1}). The determination of peak intensities, deconvolution, and calculation of integrated areas were performed using the Omnic software facilities from Nicolet.

The solid-state ^{13}C MAS−NMR analysis of all of the asphaltene samples was performed in a Brucker model Avance 400 spectrometer at 9.3 T of the magnetic field with a single-pulse excitation and magnetic angle spinning experiments, using a spinning rate of 8 KHz and ZrO_2 rotor in 4 mm prove. In all cases, TMS was used as an internal standard.

The liquid state ^{1}H and^{13}C MAS−NMR analysis of the original asphaltene samples was performed in a Jeol Model Eclipse 300, with a magnetic field of 7.04 T. The asphaltene sample was prepared as a 100 mg/cm^3 CDCl^3 solution.

(17) Al-Muhareb, E. M.; Karaka, F.; Morgan, T. J.; Herod, A. A.; Bull, I. D.; Kandiyoti, R. *Energy Fuels* **2006**, *20*, 1165.
(18) Nali, M.; Corana, F.; Montanary, L. *Rapid Commun. Mass Spectrom.* **1993**, *7*, 684–687.
(19) Trejo, F.; Ancheyta, J. *Ind. Eng. Chem. Res.* **2007**, *46* (3), 7571.
(20) Yasar, M.; Trauth, D. M.; Klein, M. T. *Energy Fuels* **2001**, *15*, 504.
(21) Andrésen, J. M.; Strohm, J. J.; Sun, L.; Song, C. *Energy Fuels* **2001**, *15*, 714.
(22) Song, C.; Lai, W.-C.; Schobert, H. H. *Ind. Eng. Chem. Res.* **1994**, *33*, 534.
(23) Speight, J. G. Asphaltenes and asphalts I. *Developments in Petroleum Science*; Yen, T. F., Chilingarian, G. V., Eds.; Elsevier: Amsterdam, The Netherlands, 1994; Vol. 40, Chapter 2.
(24) Gray, M. R.; McCaffey, W. C. *Energy Fuels* **2002**, *16*, 756.
(25) Yen, T. F.; Wu, W. H.; Chilingar, G. V. *Energy Sources* **1984**, *7*, 203.
(26) Scotti, R.; Montanari, L. In *Structures and Dynamics of Asphaltenes*; Mullins, O. C., Sheu, E. Y., Eds.; Plenum Press: New York, 1998; Chapter 3.

(A)

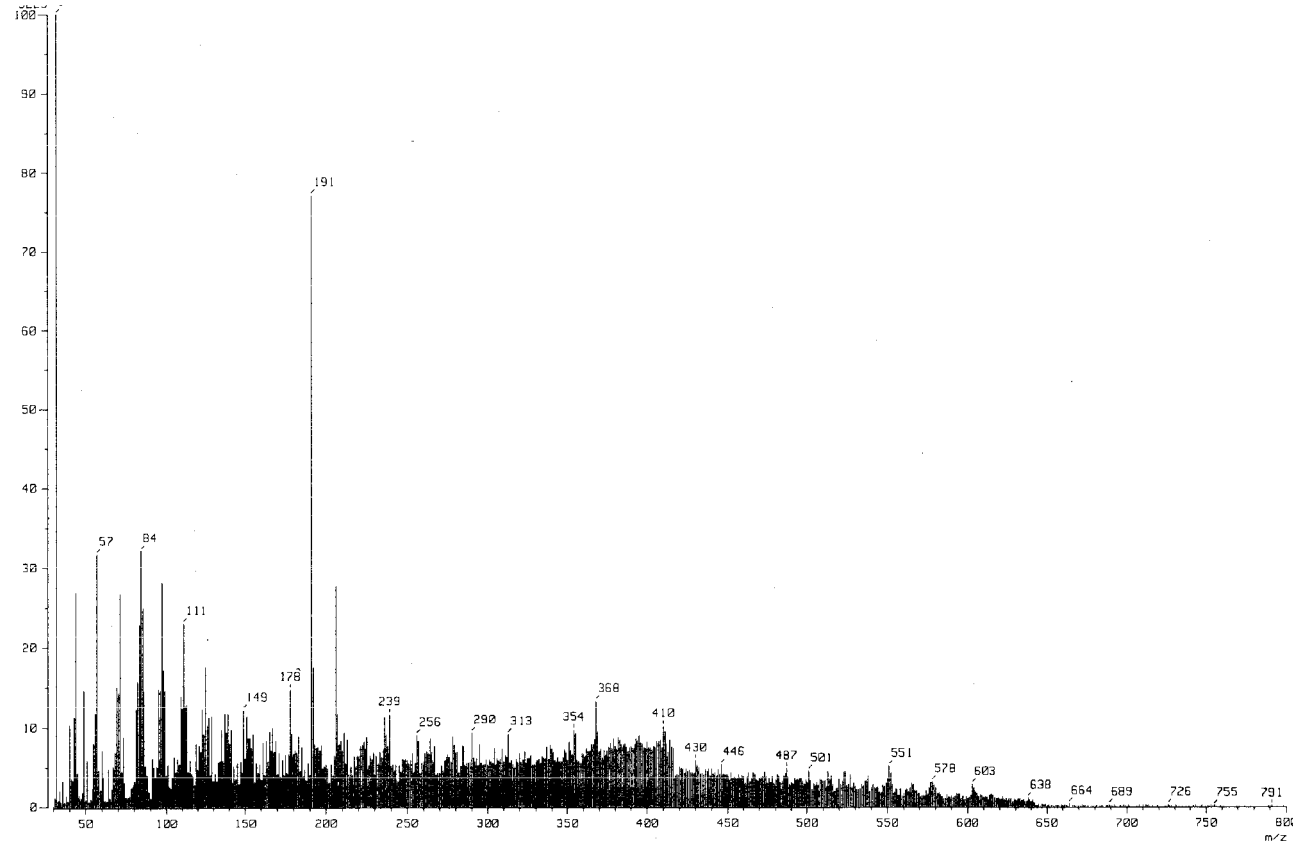
100
90
80
70
60
50
40
30
20
10
0
57
84
111
149
178
191
239
256
290
313
354
368
410
430
446
487
501
551
578
603
638
664
689
726
755
791
50
100
150
200
250
300
350
400
450
500
550
600
650
700
750
800
m/z

(B)

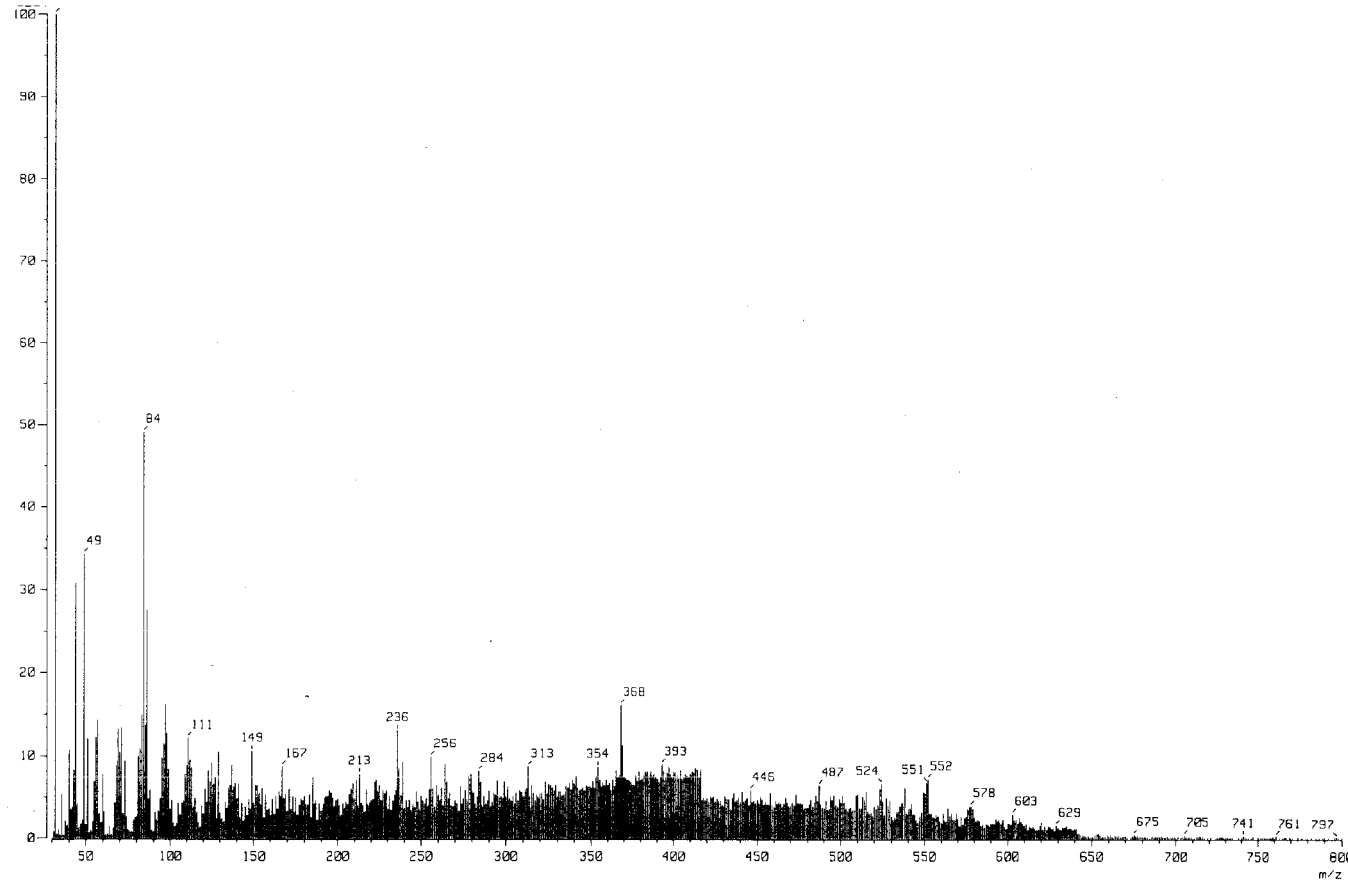
100
90
80
70
60
50
40
30
20
10
0
49
84
111
149
167
213
236
256
284
313
354
368
393
446
487
524
551
552
578
603
629
675
705
741
761
797
50
100
150
200
250
300
350
400
450
500
550
600
650
700
750
800
m/z

Figure 1

(C)

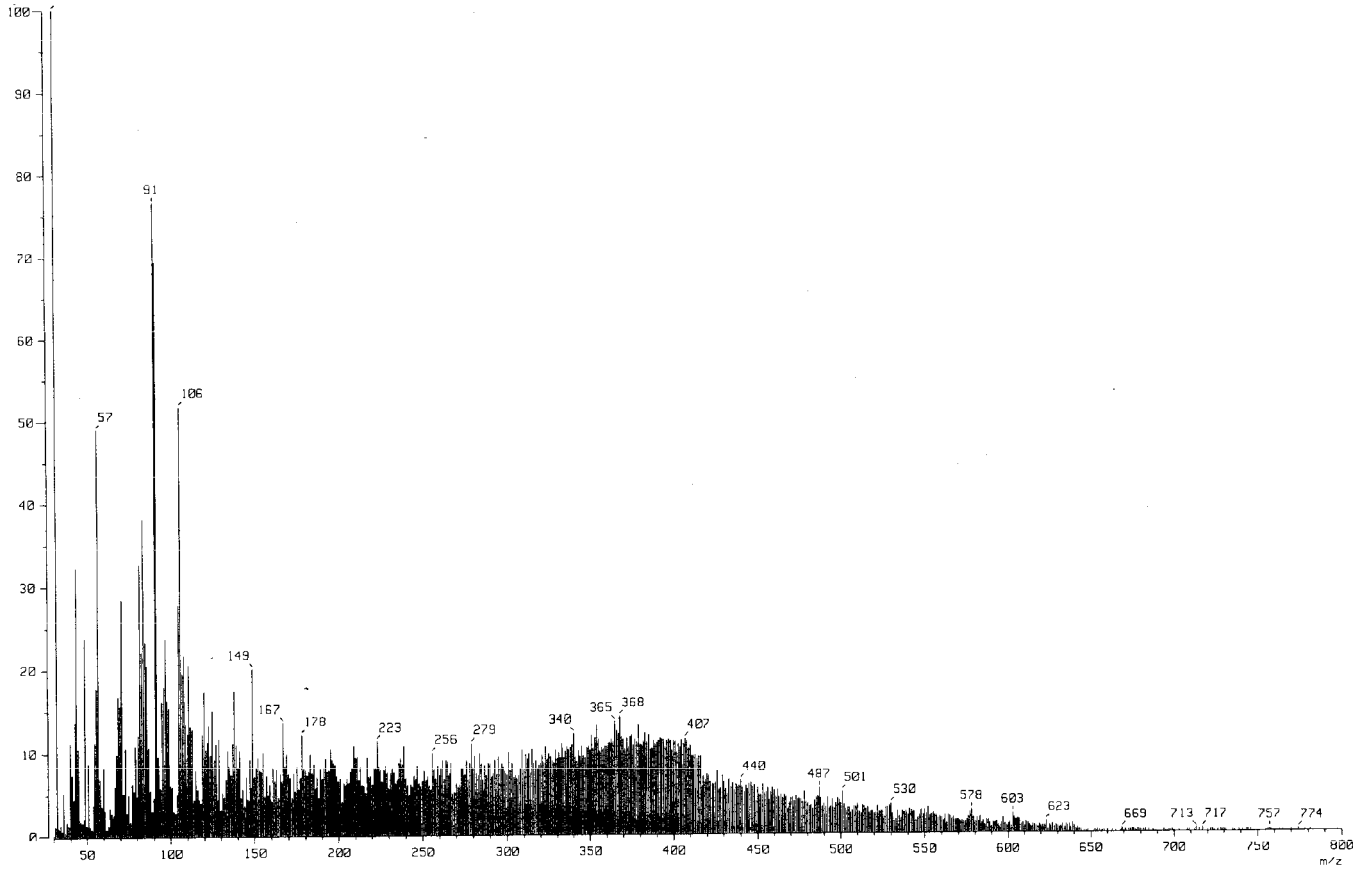
100
90
80
70
60
50
40
30
20
10
0
91
106
57
149
157
178
223
255
279
340
365
368
407
440
487
501
530
578
603
623
669
713
717
757
774
50
100
150
200
250
300
350
400
450
500
550
600
650
700
750
800
m/z

(D)

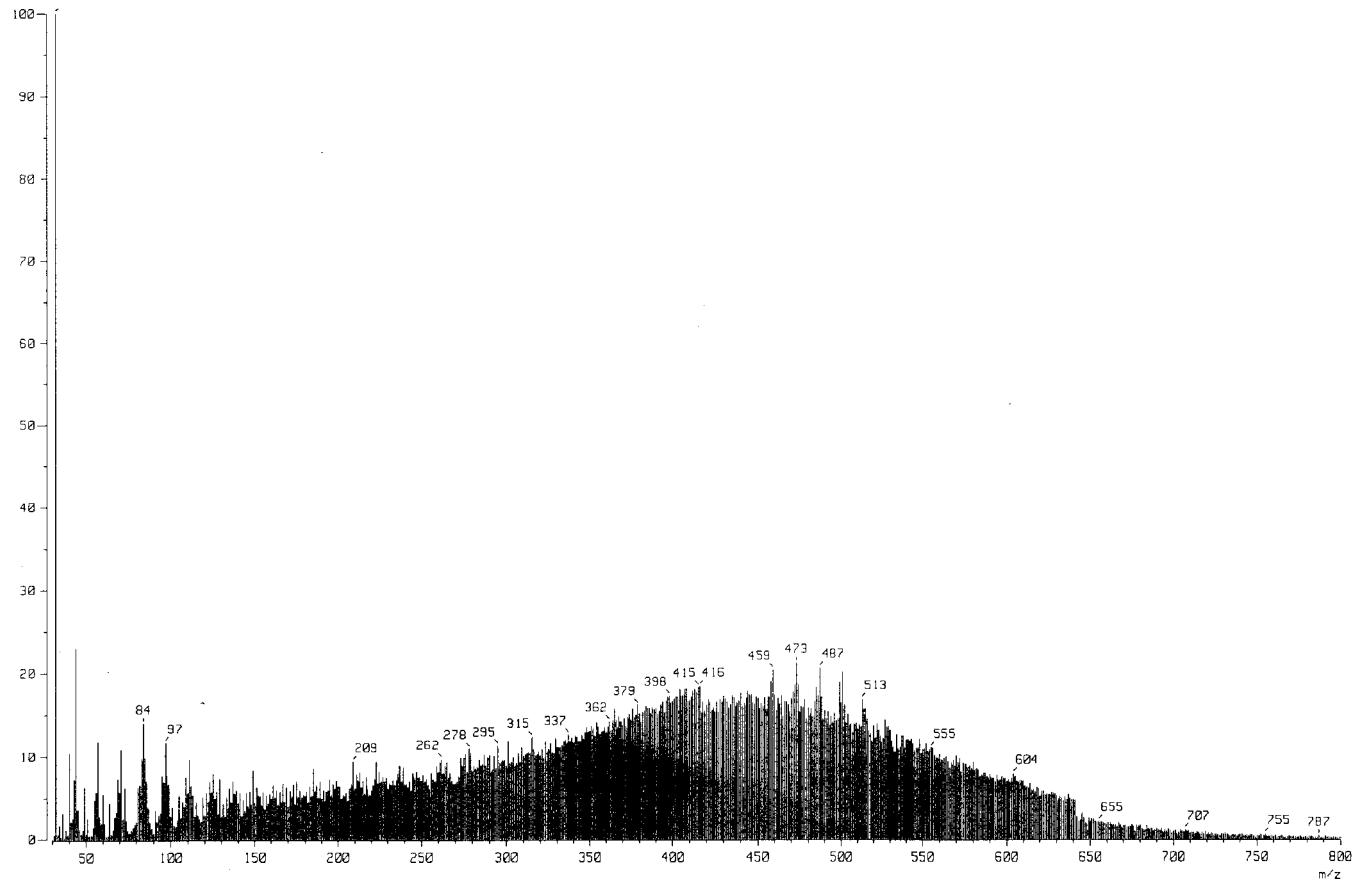
100
90
80
70
60
50
40
30
20
10
0
84
97
209
262
278
295
315
337
362
379
398
415
416
459
473
487
513
555
604
655
707
755
787
50
100
150
200
250
300
350
400
450
500
550
600
650
700
750
800
m/z

Figure 1

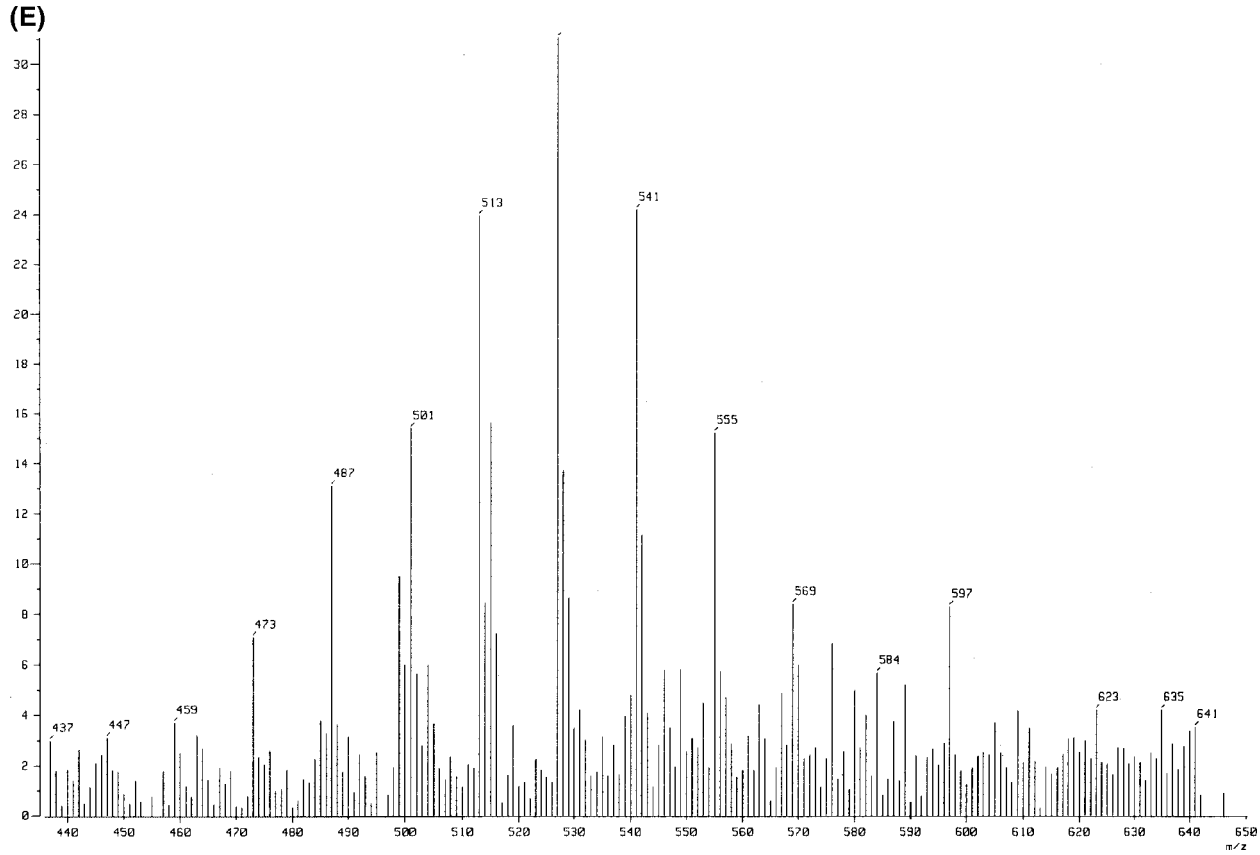

Figure 1. EIMS ion scan of Maya asphaltene of the (A) A sample, (B) B sample, (C) C sample, (D) D sample, and (E) porphyrin sample, respectively.

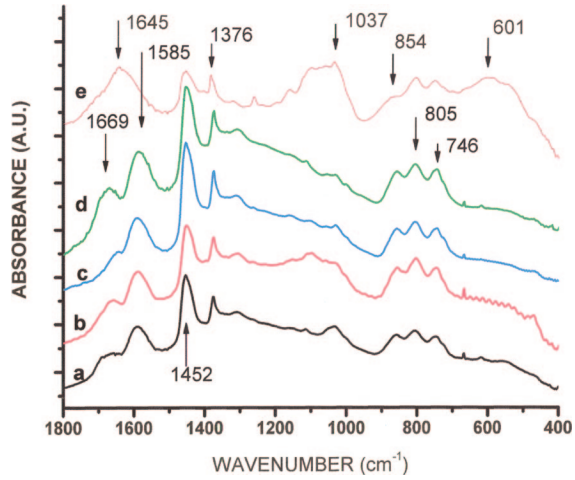

Figure 2. Infrared spectra of five asphaltene samples (A−E, respectively) identified by FTIR technique.

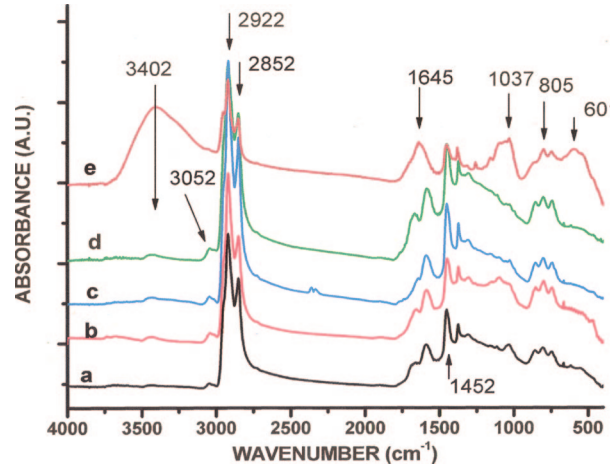

Figure 3. Region 1800−1600 cm^{-1} of infrared spectra of five asphaltene samples (A−E, respectively).

The Maya asphaltene samples are referred to as: A, initial asphaltene; B, asphaltene after pyrolysis at 350 °C with 20 min of temperature exposition; C, asphaltene after pyrolysis at 350 °C (30 min); D, asphaltene after pyrolysis at 400 °C (30 min); and E, asphaltene after pyrolysis at 450 °C (30 min).

The Maya maltene samples are referred as: Am, initial maltene; Cm, maltene after pyrolysis at 350 °C; Dm, maltene after pyrolysis at 400 °C; and Em, maltene after pyrolysis at 450 °C. All maltene pyrolysis experiments have been performed with 30 min of temperature exposition.

For the TGA and DTA of the initial maltene sample, Perkin-Elmer equipments were used: models TGA-7 and DTA-7, respectively.

Results and Discussion

The ratio of the Maya asphaltene fractions after pyrolysis at different temperatures was reported in our previous work.[3] The results are briefly resumed in Table 1.

EIMS of the Asphaltene Samples. The results of EIMS of the Maya asphaltene samples are shown in Figure 1. The molecular-weight distributions of the pyrolyzed samples are different if compared to those of the original sample.

When the spectra of the initial asphaltene and asphaltene obtained at different pyrolysis temperatures are compared, one

(27) Hauser, A.; Bahzad, D.; Stanislaus, A.; Behbahani, M. *Energy Fuels* **2007**, *22*, 449.

Table 2. Intensities of FTIR Absorbency of the Asphaltene Samples, *I*, and Values of the Length of the Alkyl Side Chains, *R*[a]

samples	I_{3050}	I_{2957}	I_{2927}	I_{2850}	I_{1600}	I_{1458}	I_{1383}	$I_{926-665}$	*R*
A	0.02	0.24	0.41	0.22	6.89	0.21	0.04	0.07	2.12
B	0.05	0.48	0.99	0.44	13.12	0.40	0.13	0.14	2.57
C	0.04	0.31	0.71	0.27	14.86	0.36	0.11	0.17	2.87
D	0.02	0.13	0.30	0.10	4.13	0.11	0.05	0.06	2.76
E	0.04	0.09	0.13	0.08	0.87	0.04	0.04	0.04	1.86

[a] The peak height units are arbitrary.

can detect some changes of the mass ion distributions.[29–31] The presence of some ions in the mass spectra also changes: the spectrum of the D sample (Figure 1B) has the most evident differences with respect to other samples and contains more abundant ions in the region from 150 to 650 amu. Only in this spectrum, it is possible to observe the most abundant ions at *m*/*z* 459, 473, 487, 501, and 515 of the homologous series, tentatively assigned to the asphaltene porphyrins, because the same series of ions has been found in the separated fraction of vanadium porphyrin of the original Maya asphaltene sample (up to *m*/*z* 555, as seen in Figure 1E). It sounds reasonable because the porphyrins are cross-linked to other aromatic fused ring systems,[32,33] and they may appear on the 350−450 °C EIMS spectra because of the breaking of these linkages. At the same time, the smallest molecules of asphaltene are of porphyrin size.[34,35] The ions of *m*/*z* 487 and 501 are present at almost all spectra; however, they do not look like a well-defined homologous series.

As was mentioned,[23] the nickel and vanadium occur as porphyrins, but whether or not these are an integral part of the asphaltene structure is not known; besides, it has been noted that the organic nitrogen in the asphaltenes invariably undergoes a thermal reaction to concentrate in the nonvolatile coke, and only 1% of the nitrogen is lost during the thermal treatment.[23] Our result agrees with the conclusion of Hauser et al.:[27] Asphaltenes have a bimodal composition, that is, thermally steady and easily converted parts. As we just observed in our study, the thermally steadier fraction of asphaltene is most likely the fraction with porphyrin compounds. These conclusions, together with the proposed structure of asphaltene (which incorporated metal ions)[36] and the structure recently proposed by Trejo et al.,[19] can suggest the idea of the porphyrin-based asphaltene molecule. This idea may be supported by some common observations: the asphaltenes of different origins often have similar properties, which are independent of molecular weight, chemical compositions, and metal ion content. For instance, one of the most remarkable similarities between different asphaltene samples is their almost identical ratio of hydrogen to carbon atoms, H/C = 1.15 ± 0.5.[37] This detail may lead to a general belief that the asphaltenes do have a characteristic chemical composition and structure,[38] which may permit a more meaningful description than that of just a solubility class.[39] It also agrees with a detail that the maltene molecules sometimes have a greater molecular weight and a smaller metal content than some asphaltene fractions; it is known that in maltene the Ni content is 10 times and the V content is 15 times lower if compared to the asphaltene content.[38]

As we have observed, the asphaltene fraction obtained at 450 °C is the smallest fraction and with the highest porphyrin molecules content. Tentatively, this fraction represents the thermally most stable asphaltene among the Maya asphaltene pyrolysis products.

Finally, it is worth mentioning the steps in intensity of the spectra at about *m*/*z* 420 at all parts of Figure 1. Tentatively, such behavior may be attributed to the restrictions of the EIMS method. As was recently stated by Herod et al.,[40] many of the techniques optimized for the analysis of material up to ∼450 amu cannot be readily adapted for examining samples that contain higher molar mass (MM) materials. Namely, mass spectroscopy methods cannot easily define the upper limits of complex fractions, because an absence of signal does not

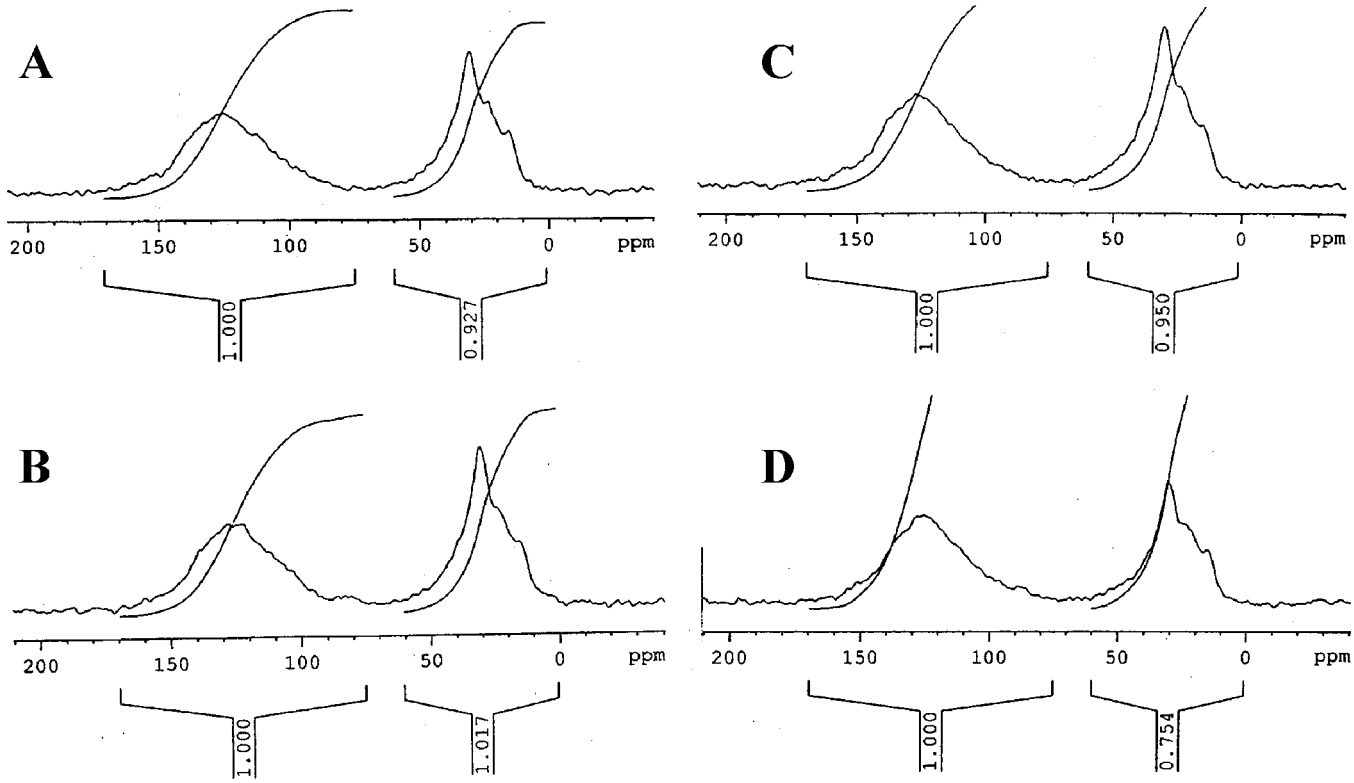

Figure 4. Solid-state ^{13}C MAS−NMR spectra of Maya asphaltene samples (A−D, respectively).

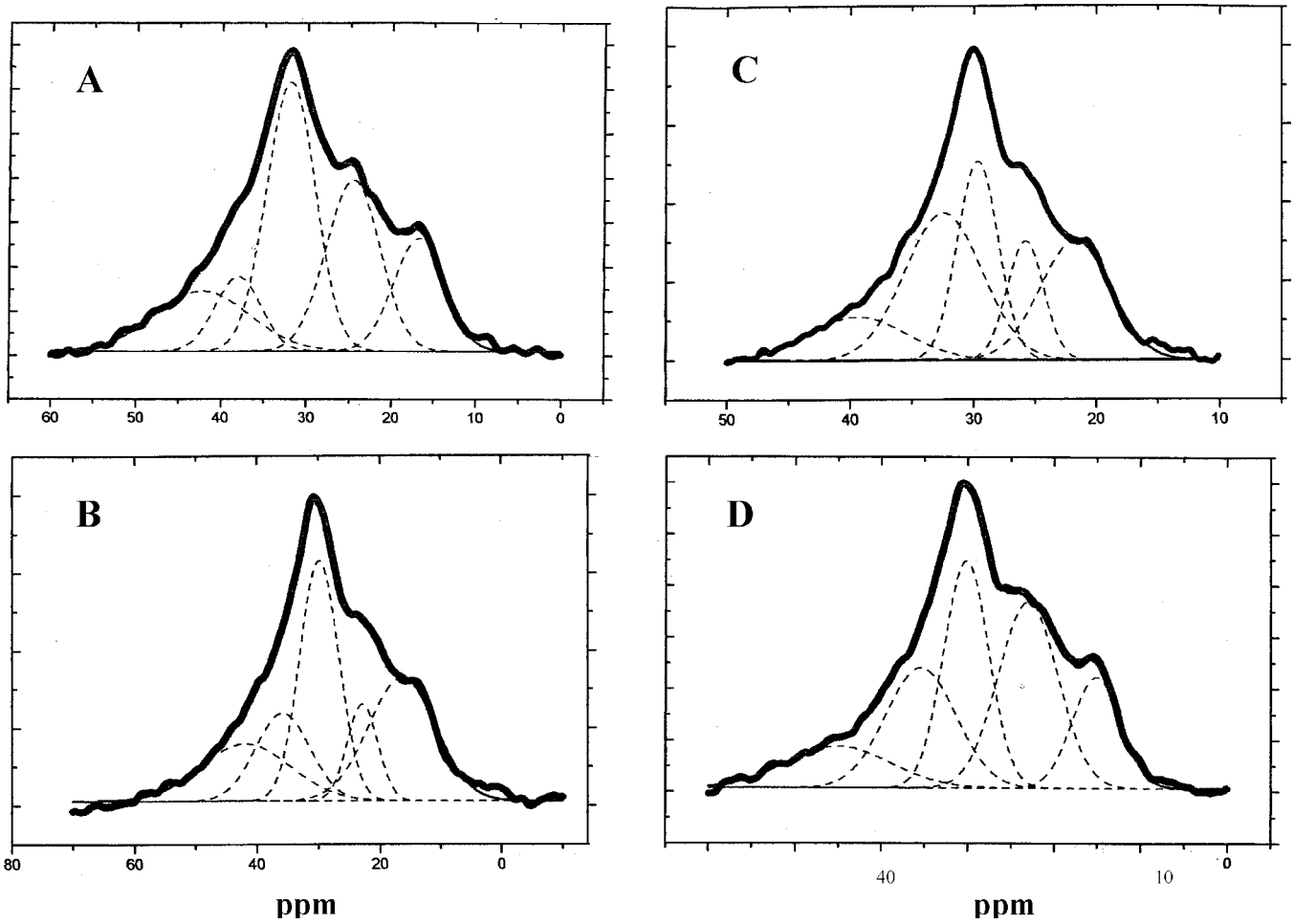

Figure 5. Aliphatic zone (60−0 ppm) of solid-state ^{13}C MAS−NMR spectra of Maya asphaltene samples (A−D, respectively).

Table 3. Average Areas of the Peaks in the Aliphatic Zone (60−0 ppm) of Solid-State ^{13}C MAS−NMR Spectra of the Maya Asphaltene Samples A−D

samples	1	2	3	4	5
A	15.7	24.7	35.0	9.2	15.4
B	27.2	9.7	30.7	15.6	16.8
C	23.2	12.0	22.4	30.9	11.5
D	13.7	28.2	25.9	21.3	10.9

necessarily mean an absence of material. Instead, it may simply indicate that the limit of ionization with an increasing MM under the particular conditions may have been reached. In ref 40, authors suggested analysis and a comparison of MM from several independent analytical methods. Thus, to obtain an exact interpretation of the step around 420 amu, further investigation is required.

FTIR Characterization of the Asphaltene Samples. In Figures 2 and 3, the comparison of the FTIR spectra of the original and asphaltene obtained at different temperatures shows that the functional groups in the samples are essentially similar, although they do have different intensities of the bands (see Table 2).

The broad absorption bands in the 3200−3450 cm^{-1} region presented in all samples is a characteristic of the O−H stretching vibration and/or N−H stretching frequencies.[41] These bands are more abundant for the E sample, indicating that the concentration of these groups in the asphaltene fractions increases under heating. The absorption band of the C−H aromatic stretching vibration, above 3000 cm^{-1}, is rising at 350 and 450 °C and less intense at 400 °C (Table 2).

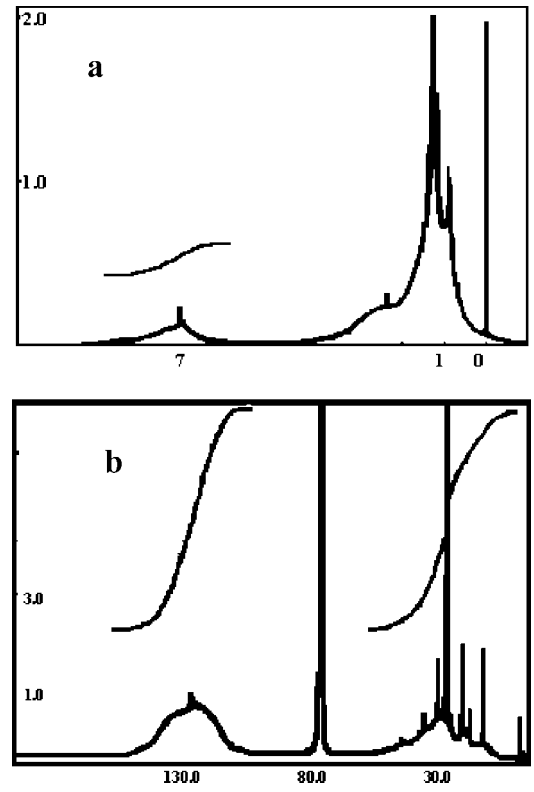

Figure 6. Solution-state (a) ^{1}H and (b) ^{13}C NMR spectra of the original Maya asphaltene sample.

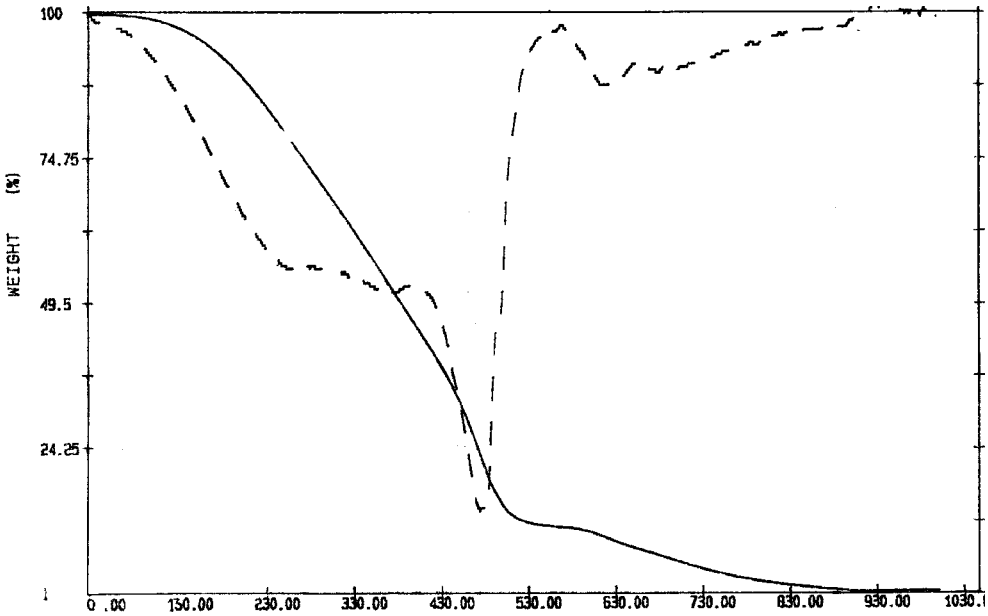

Figure 7. TGA of Maya maltene under the nitrogen atmosphere. The scanning rate is 10 °C/min.

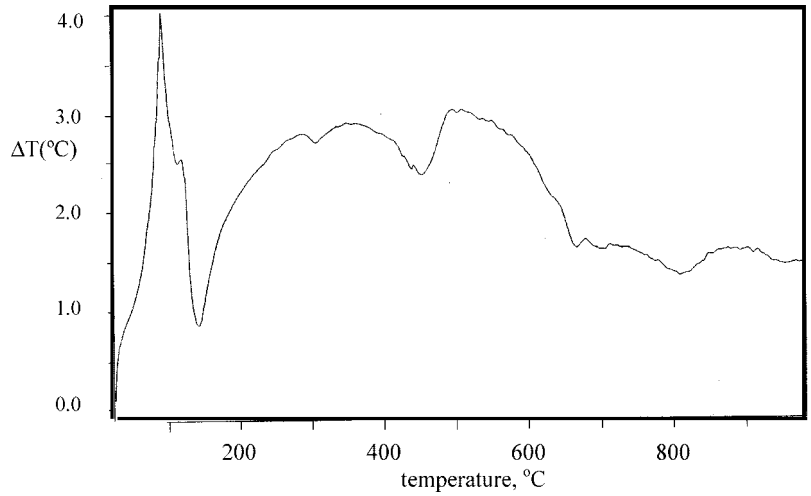

Figure 8. Results of DTA of Maya maltene. The flow rate is 10 °C/min, and the peak corresponds to 100 and 500 °C.

The alkyl side chains on the condensed aromatic ring sheets are related to the signals around 2850−3000, 1460, and 1380 cm^{-1}. They are increased for the samples A and B and decreased up to the E sample. Similar trends are obtained for the intensities of bands at 2957 and 2927 cm^{-1}; i.e., at 350 °C (samples B and C), the intensities of these bands increase if compared to the original sample, and they decrease significantly at 400 °C.

To evaluate the length of the alkyl side chains, we calculate the molar ratios of CH_2 and CH_3 groups of the asphaltene samples[26]

$$R = nCH_2/nCH_3 = KI_{2927}/I_{2957}, \quad \text{where } K = 1.243$$

Obviously, the higher R value corresponds to the longer side chain. Our results presented in Table 2 show that the E sample possesses the shortest alkyl side chains.

As expected, taking into account the low content of oxygen in the original asphaltene sample (elemental analysis results), the data do not exhibit a noticeable carbonyl group absorption band. However, the more detailed analysis of the region 1600−1800 cm^{-1} in Figure 3 permits us to observe some important features. Namely, the aromatic $\gamma_{C=C}$ band absorption at 1600 cm^{-1}, which is often interpreted as a result of the condensation of aromatic rings C,[42] increased almost 2 times after pyrolysis at 350 °C, while it decreased significantly at 400 and 450 °C. The similar trends were reported for Athabasca

(28) García-Arellano, H.; Buenrostro-Gonzalez, E.; Vazquez-Duhalt, R. *Biotechnol. Bioeng.* **2004**, *85*, 790.
(29) Morgan, T. J.; Millan, M.; Behrouzi, M.; Herod, A. A.; Kandiyoti, R. *Energy Fuels* **2005**, *19*, 164.
(30) Madrali, E. S.; Wu, F.; Xu, B.; Herod, A. A.; Kandiyoti, R. *Energy Fuels* **1995**, *9*, 269.
(31) Sato, S.; Takanohashi, T. *Energy Fuels* **2005**, *19*, 1991.
(32) Andersen, S. I.; Keul, A.; Stenby, E. H. *Pet. Sci. Technol.* **1997**, *15* (7−8), 611.
(33) Andersen, S. I. *J. Liq. Chromatogr. Relat. Technol.* **1994**, *17* (19), 4065.
(34) Groenzin, H.; Mullins, O. C. *J. Phys. Chem. A* **1999**, *103*, 11237.
(35) Groenzin, H.; Mullins, O. C. *Energy Fuels* **2000**, *14*, 677.
(36) Trauth, D. M.; Yasar, M.; Neurock, M.; Nigam, A.; Klein, M. T.; Kukes, S. C. *Fuel Sci. Technol.* **1992**, *10*, 1161.
(37) Watson, B. A.; Barteau, M. A. *Ind. Eng. Chem. Res.* **1994**, *33*, 2358.
(38) Speight, J. G. *The Chemistry and Technology of Petroleum*, 2nd ed.; Marcel Dekker, Inc.: New York, 1991.
(39) Ibrahim, H. H.; Idem, R. O. *Energy Fuels* **2004**, *18*, 1354–1369.
(40) Herod, A. A.; Bartle, K. D.; Kandiyoti, R. *Energy Fuels* **2007**, *21*, 2176–2203.
(41) Calemna, V.; Iwanski, P.; Nali, M.; Scotti, R.; Montanari, L. *Energy Fuel* **1995**, *9*, 225.
(42) Mansuy, L.; Landais, P.; Ruau, O. *Energy Fuels* **1995**, *9*, 691.

asphaltene pyrolyzed at 400 °C.[41] The next band at 1645 cm^{-1} can be assigned to $\gamma_{C=C}$ conjugated stretching vibration (1600−1650 cm^{-1}). These bands have major intensity for the E sample and are absent for the C and D samples. The results for the bands at 1458 and 1383 cm^{-1} that represent the CH bending vibrations of aliphatic and naphthenic rings are similar: they decrease from the B to C sample. The peaks in the region 1230−1037 cm^{-1} indicate the presence of different sulfur-containing compounds[16] and are more abundant for the D sample.

The spectra indicate that the intensities in the region 926−665 cm^{-1} (H atoms out-of-plane vibrations on aromatic rings) increase from the A to C sample but decrease for the D and E samples. Analyzing the results of Table 2, one can also observe that intensities of almost all peaks have a high value at 350 °C (samples B and C) and then decrease at 400 and 450 °C (samples D and E). The increase of the pyrolysis time (from the B to C sample) leads to a decrease of most peak intensities. Our results resemble those of ref,[33] where no noticeable bands in this region were found for Athabasca asphaltene. We also observe that in this region the samples D and E have the smallest values, because the decarboxylation and double bonds breaking occur at temperatures higher than 400 °C.

In summary, the obtained results reveal that (i) the aliphatic bands are increased up to 350 °C and decreased again at 400 and 450 °C with respect to the original sample, (ii) the carbonyl groups intensities increase at 450 °C, and (iii) the aromatic content increases up to 350 °C and again decreases at temperatures of 400 and 450 °C.

Solid-State ^{13}C MAS−NMR Analyses of the Asphaltene Samples. The quantitative solid-state MAS−NMR has been used to evaluate the degree of condensation and substitution of aromatic rings of the Maya asphaltene samples. As seen in Figure 4, the spectrum is clearly divided into two abundant peaks centered approximately at 160−100 ppm (aromatic region) and 60−0 ppm (aliphatic region).

The total aromatic carbon abundances, *F*, have been derived from the integration of the NMR band at 160−90 ppm. The Maya asphaltene samples show the same values of aromatic condensation for the initial temperature and asphaltene obtained at different temperatures ($F = 1.00$); therefore, the sample has the same size of polycondensed aromatic rings. These *F* values are similar to those obtained for the asphaltene of different origins.[23] The average number of polycondensed aromatic rings (if the *F* value is 1.0) has been estimated to be between 5 and 7.[39]

The most significant changes are observed in the aliphatic zone of spectra presented in Figure 5 and Table 3. The saturated carbon region (65−10 ppm) shows the changes occurring at two directions. The value of integration of the aliphatic region increases from 0.927 (A sample) to 1.017 (B sample) and decreases to 0.950 (C sample), and 0.754 (D sample), which is in good agreement with IR results. The f_a value, fraction of the aromatic carbon, was estimated from the ratio of the area of the aromatic region (160−100 ppm) to the summed areas of the aromatic and aliphatic (0−60 ppm) regions. This value for the asphaltene samples is increased with the temperature as follows: 0.51 for the A sample, 0.52 for the B sample, 0.57 for the D sample, and 0.50 for the C sample.

The deconvolution of the peaks of the aliphatic zone of the spectrum in Figure 5 and Table 3 permits us to observe some area changes of linear alkyl chains, which occur with temperature.[42,43] The first peak (45 ppm), tentatively assigned to quaternary alkyl groups and/or αCH_2, is increased from the A to B sample and decreased to the C and D samples. The second peak (37.3 ppm) of methylene in the α position with respect to aromatic rings has the highest and lowest values for the D and B samples, respectively. The major third peak (30 ppm), assigned to paraffinic methylene of long alkyl chains (γCH_2), is decreased up to the C sample and slightly increases to the D sample. The fourth peak (25 ppm) of the methyl on the end of alkyl chains has the lowest and highest values for the A and C samples, respectively. Finally, the peak 5 (25−10 ppm) of cyclic CH_2 and lateral alkyl chains increases from the A to B sample and decreases from the C to D sample. These results reflect the similar temperature changes of the asphaltene structure if compared to those obtained by means of the FTIR technique.

Solution-State ^1H and ^{13}C NMR Analyses of the Original Asphaltene Sample. The solution-state ^1H and ^{13}C MAS−NMR analyses of the initial Maya asphaltene have been performed, and the results are presented in Figure 6. The ^1H MAS−NMR spectra have the extensive bands of the aromatic and saturated regions. This may be attributed to a great number of asphaltene compounds with very different structure composition. The ^1H MAS−NMR spectra were deconvoluted in 4 bands: from −1.0 to 1.0 ppm, $\gamma+$ CH_3 (H_α); from 1.0 to 2.0 ppm, $\beta+$ CH_3, CH_2, and CH (H_β); from 2.0 to 4.0 ppm, α CH_3, CH_2, and CH (H_γ); and from 6.5 to 9.0 ppm, aromatic CH (H_{ar}). The ^{13}C NMR spectra have been divided into two integration regions: from 10 to 65 ppm, aliphatic C (C_{al}) and from 100 to 160 ppm, aromatic C (C_{ar}). The same aromaticity factor $f_a = 0.51$ was obtained as for the A sample by solid-state ^{13}C MAS−NMR.

Thermal Analysis of the Initial Maya Maltene Sample. The TGA technique was used to characterize the temperature profile of volatilization and decomposition of the Maya maltene sample. The results, in terms of mass loss as a function of the temperature, are given in Figure 7. It is observed that a rapid thermal decomposition begins at 215 °C and ends at 996 °C, with the maximum rate of weight loss at 475 °C. The changes of percent weight are 13.4% at temperatures from 25 to 215 °C, 75.9% from 215 to 550 °C, and 11.5% from 550 to 996 °C. Total weight loss is 100% at experimental conditions.

During the DTA experiment, Maya maltene shows a considerable decomposition at 25−670 °C, with the maximum at 100 and 500 °C (see Figure 8). These results are similar to those for Garzan resins.[15]

TGA and DTA techniques detect the changes of the percent weight of solids at the temperature range of 350−450 °C. However, the outline pyrolysis applied in this work permits us the recuperation and analysis of the pyrolysis products.

Dynamic Pyrolysis of the Initial Maya Maltene Sample. The pyrolysis temperatures of 350 and 400 °C were chosen for a comparison of Maya asphaltene[3] and maltene pyrolysis results. During thermal decomposition of the maltene at 350, 400, and 450 °C, we have obtained several groups of compounds: coke, gas, asphaltene, and maltene. Each group was separated by the solubility sequence. Product yields are given in Table 1. The increase of the temperature from 350 to 450 °C results in a decrease of unreacted maltene products and an increase of coke, asphaltene, and gas products (see Table 1). If we compare these results to those obtained from asphaltene pyrolysis, we observe less coke and asphaltene production and more maltene and gas production. Our results at 450 °C are similar to the results reported by Trauth et al.[36] for a Arabian Light maltene at 425

(43) Kotlyar, L. S.; Morat, C.; Ripmeester, J. A. *Fuel* **1991**, *70*, 90–94.

°C; however, they obtained more maltene and less gas products. This discrepancy may be due to different techniques applied, different origin of samples, slight temperature difference, and high-pressure nitrogen (up to 5 atm) applied.[44]

Conclusions

In the present work, for the first time, Maya maltene outline pyrolysis has been performed at different temperatures. As expected, the pyrolysis at higher temperatures yielded more asphaltene and coke production. The TGA data show that the maltenes are stable up to 215 °C, but after this temperature, they undergo faster conversion up to 550 °C. Complete weight loss occurs up to 996 °C. The product fractions obtained from the pyrolysis reflect the composition of original Maya maltene in a quantitative way.

The study of Maya asphaltene pyrolysis products of asphaltene fractions at 350, 400, and 450 °C is presented, and their structural parameters are compared. The structural parameters of original and pyrolyzed Maya asphaltenes are compared by applying different analytic techniques: pyrolysis, EIMS, FTIR, and liquid and solid MAS−NMR. We have found that the aliphatic region of the asphaltene molecule suffers more significant alteration by heating (at least, at 350−450 °C), if compared to the aromatic region.

EIMS analysis indicates that the asphaltenes obtained at 450 °C are the smallest fraction, however, with the highest porphyrins content. This fraction may be considered as the most thermally stable asphaltene fraction among all of the Maya asphaltene pyrolysis products.

We suppose that the asphaltene molecule, because of the presence of metal−porphyrin molecules, has a special spatial structure, with the porphyrin molecules being a core of asphaltene molecule and other aromatic and heterocyclic compounds (that are peripherically bonded with a help of the alkyl chains) being a shell. These asphaltene molecules form the micelles with maltenes, as we reported.[11]

The loss of asphaltene properties during industrial thermal treatment or pyrolysis may also be related to the transformation of spatial structure and not only to the molecular mass loss of asphaltene molecules. If we are right, this guess may explain the similar comportment of the asphaltenes of different sources. To confirm this tentative suggestion, more studies are required.

The study of asphaltene temperature modifications is important for the prevention of the asphaltene deposits during coking, cracking, and distillation. We believe, that the obtained structure details of the Maya asphaltene[3,11] and maltene will be useful for the modeling study of asphaltene agglomeration, precipitation, and production of asphaltene deposits[4–6,21,45–48] as well as prevention of the processes of coke formation in the crude oils.

Acknowledgment. We thank R. I. Conde Velazco and C. López Franco from IMP for technical support. Helpful discussions with Y. Duda are gratefully acknowledged.

EF800024P

(44) Lindeman, I.; Adams, J. Q. *Anal. Chem.* **1971**, *43*, 1245–1252.

(45) Grijalva-Monteverde, H.; Arellano-Tánori, O. V.; Valdez, M. A. *Energy Fuels* **2005**, *19*, 2416.

(46) Duda, Y.; Lira-Galeana, C. *Fluid Phase Equilib.* **2006**, *241*, 257.

(47) Aguilera-Mercado, B.; Herdes, C.; Murgich, J. *Energy Fuels* **2006**, *20*, 327.

(48) Coelho, R. R.; Hovell, I.; Monte, M. B. D.; Middea, A.; de Souza, A. L. *Fuel Process. Technol.* **2006**, *87*, 325.